

# Excessive proliferation and apoptosis of parathyroid cells contribute to primary hyperparathyroidism in rabbit model

Jing-tao Bi <sup>1</sup>, Rong-jie Bai,<sup>2</sup> Hui-li Zhan,<sup>2</sup> Zhan-hua Qian,<sup>2</sup> Li-hua Gong,<sup>3</sup> Ya-qi Liu,<sup>1</sup> Zhi-xue Zheng,<sup>1</sup> Xuan Cai<sup>1</sup>

<sup>1</sup>Department of General Surgery, Beijing Jishuitan Hospital, Beijing, China

<sup>2</sup>Department of Radiology, Beijing Jishuitan Hospital, Beijing, China

<sup>3</sup>Department of Pathology, Beijing Jishuitan Hospital, Beijing, China

## Correspondence to

Rong-jie Bai, Department of Radiology, Beijing Jishuitan Hospital, Beijing 100035, China; bairongjie@126.com

Accepted 24 February 2022  
Published Online First  
22 March 2022

## ABSTRACT

To explore the molecular pathogenesis of primary hyperparathyroidism (PHPT), we investigated the proliferation and apoptosis of parathyroid cells in a rabbit model of diet-induced PHPT. A total of 120 adult Chinese rabbits were randomly divided into normal diet (Ca:P, 1:0.7) group (control group) or a high-phosphate diet (Ca:P, 1:7) group (experimental group). The thyroid and parathyroid complexes were harvested for 1-month interval from month 1 to month 6. The expression of proliferation markers, including proliferating cell nuclear antigen (PCNA) and cyclin-D1, and B cell lymphoma-2 (Bcl-2), were evaluated by immunohistochemistry in thyroid and parathyroid tissues. Apoptosis was quantified by DNA-fragment terminal labeling. Our results demonstrated that parathyroid cells in the experimental group started proliferating from the end of the 2nd month, the expression of PCNA, Bcl-2, and cyclin-D1 were significantly higher in the PHPT group than those of the control group ( $p < 0.05$ ). Furthermore, the apoptosis index (AI) was positively correlated with the glandular cell count and expression of PCNA in the 6th month in the PHPT group. Overall, our results suggested that excessive proliferation and apoptosis of parathyroid cells may contribute to the pathogenesis of PHPT through PCNA-related, Bcl-2-related, and cyclin-D1-related pathways.

## INTRODUCTION

Primary hyperparathyroidism (PHPT) is an endocrine disease that is relatively common in Europe and America, with an incidence of 8 in 100 000.<sup>1</sup> PHPT has a variety of clinical manifestations, an insidious onset and a harmful pathology. However, its pathogenesis has not yet been fully clarified, leading to early misdiagnoses or missed diagnoses. Therefore, in-depth research into the pathogenesis of PHPT is necessary, especially the basic mechanisms of PHPT.<sup>1</sup> Previous studies have shown that the stability of the internal environment in multicellular organisms is maintained by a balance between cell proliferation and apoptosis.<sup>2</sup> If the balance is disrupted, the number of cells in the organism will abnormally increase or decrease, leading to the occurrence of disease. The proliferating cell nuclear antigen (PCNA) provides replicative

## Significance of this study

### What is already known about this subject?

- ⇒ A rabbit model of primary hyperparathyroidism (PHPT) can be induced by high phosphate diet.
- ⇒ The B cell lymphoma-2 (Bcl-2) protein in etiopathogenesis of hyperplasia of the parathyroid gland while PCNA might be a useful marker for differentiating adenoma from early hyperplasia in primary hyperparathyroidism cases.
- ⇒ Apoptosis plays a crucial role in the suicide and turnover of cells in various tumors.
- ⇒ The abnormal accumulation of B-catenin in the nucleus of parathyroid adenoma may start the transcription of cyclin-D1 gene, thus contributing to parathyroid cell proliferation and differentiation.

### What are the new findings?

- ⇒ Excessive proliferation and apoptosis of parathyroid cells might contribute to the pathogenesis of PHPT, and that PCNA, Bcl-2, and cyclin-D1 might play key roles in this process.
- ⇒ The imbalance of parathyroid cell proliferation and apoptosis may be the main mechanism of PHPT in the rabbit model of PHPT.

### How might these results change the focus of research or clinical practice?

- ⇒ This study provides the groundwork for using the rabbit PHPT model to elucidate its pathogenesis and develop treatment strategies.

DNA polymerases in eukaryotic cells.<sup>3</sup> Subsequent studies showed that PCNA in mammalian cells interacts with partners involved in DNA repair, DNA translation, chromatin remodeling, cell cycle regulation, and other metabolic pathways.<sup>4</sup> B cell lymphoma-2 (Bcl-2) prolongs cell survival and blocks apoptosis. Cyclin-D1 is an important positive regulator of the cell cycle, which has increasingly become a focus in the study of tumor development.<sup>3</sup> Overexpression



© American Federation for Medical Research 2022. No commercial re-use. See rights and permissions. Published by BMJ.

**To cite:** Bi J, Bai R, Zhan H, et al. *J Invest Med* 2022;**70**:1392–1398.

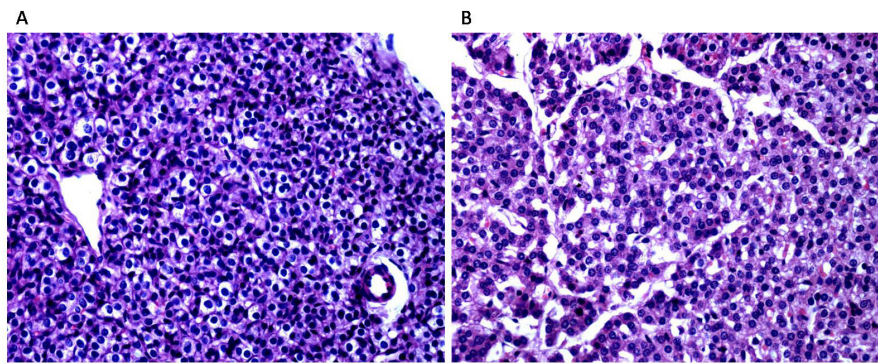


**Figure 1** H&E staining (×400) for parathyroid tissue section. (A) From a rabbit in control groups with no significant hyperplasia. (B) From a rabbit after receiving the high-phosphate diet for 6 months. There are hyperplasia with significant increase of parathyroid cell count and parathyroid gland volume in experimental groups.

of the cyclin gene is the main molecular mechanism of parathyroid tumors.<sup>5</sup> However, the roles of PCNA, Bcl-2, and cyclin-D1 in the dynamic pathogenesis of PHPT remain unclear. In a previous study, we successfully established an animal model of PHPT.<sup>6,7</sup> This model was used to explore the relationship between the proliferation and apoptosis of parathyroid cells and their role in the development of PHPT, which may provide the theoretical basis for the study of PHPT mechanisms. That animal model of PHPT was successfully established by feeding rabbits with a high-phosphorus diet.<sup>6,7</sup> The animal model of PHPT was then used to evaluate PCNA, Bcl-2, and cyclin-D1 and to examine the proliferation and apoptosis processes in the parathyroid.

## MATERIALS AND METHODS

### Experimental animals

In total, 120 healthy adult Chinese white rabbits (60 of each sex), weighing 2.0–2.5 kg and aged 10–12 months, were raised in cages.

### Main reagents and instruments

The main reagents included PCNA immunohistochemical staining kit (Boster, California, USA); Bcl-2 immunohistochemical staining kit (Boster); cyclin-D1 immunohistochemical staining kit (Boster); in situ apoptosis detection kit (Boehringer Mannheim); and 3,3N-diaminobenzidine tetrahydrochloride (DAB) color-development kit (Beijing Zhongshan). The main instruments included a microtome (model RM2235, Leica, Germany), an Olympus BX-51 light microscope (Olympus, Japan), an Olympus microdigital camera (Olympus), and an HMIAS-2000 color pathology

analysis system (Tongji Medical College, Huazhong University of Science and Technology, Wuhan, China).

### Preparation of the rabbit model of PHPT

At 1 week before experiment and the end of the first month to the sixth month into the experiment, blood samples were retaken from ear veins of all experimental animals to determine the blood calcium and phosphorus levels using clinical biochemical analyzer (spectrophotometry), and blood parathyroid hormone (PTH) levels were determined by radioimmunoassay. Meanwhile, routine whole-body bone X-ray examination was performed to detect bone lesions and abnormal calcium and phosphorus metabolism. The 120 experimental animals were randomly divided into an experimental group and a control group ( $n=60$  in each group). According to the feeding schedule, the control and experimental groups were each further divided into six groups ( $n=10$  in each group), labeled the first-month to sixth-month groups, respectively. The control group was fed a normal diet (Ca:P, 1:0.7), while the experimental group was fed a high-phosphate diet (The concentration of calcium and phosphorus in the solution was 0.6% and 4.2%, respectively. The ratio of them was 1:7.) according to the previous study.<sup>6</sup> The animal model for PHPT was successfully established as previously reported.<sup>7</sup> The serum calcium levels increased, and serum phosphorus levels decreased in the experimental groups at the end of 4, 5, and 6 months, respectively, which was a typical feature of PHPT.

### Specimen collection

In the first, second, third, fourth, fifth, and sixth months, rabbits in the experimental and control groups were

**Table 1** Comparison of parathyroid gland cell numbers between control and experimental groups on months 1, 2, 3, 4, 5, and 6

|                              | Group | Month      |             |            |            |            |            |
|------------------------------|-------|------------|-------------|------------|------------|------------|------------|
|                              |       | 1          | 2           | 3          | 4          | 5          | 6          |
| Parathyroid cells            | C     | 410.8±19.5 | 416.9±31.8  | 417.4±20.3 | 412±23.8   | 427.5±26.2 | 427.6±26.1 |
|                              | E     | 403.6±7.5  | 574.7±116.2 | 705.5±56.7 | 711.2±24.3 | 764.6±66.3 | 810.4±46.4 |
| t value                      |       | 1.086      | −4.142      | −15.132    | −27.794    | −14.954    | −22.734    |
| P value                      |       | 0.292      | 0.001       | <0.001     | <0.001     | <0.001     | <0.001     |
| Data are mean±SEM.           |       |            |             |            |            |            |            |
| C, control; E, experimental. |       |            |             |            |            |            |            |

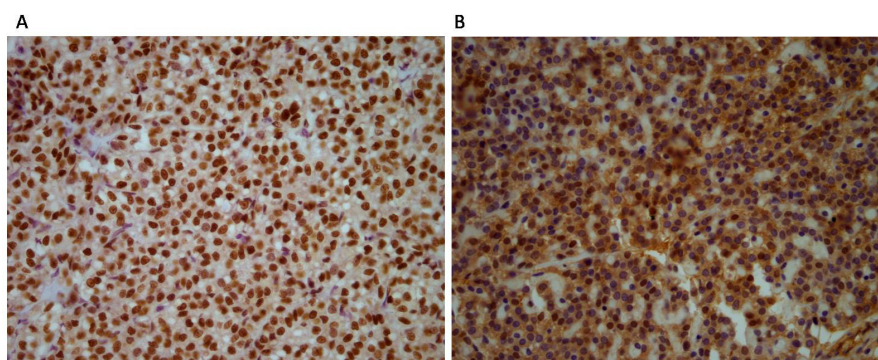


**Figure 2** Proliferating cell nuclear antigen (PCNA) protein expression ( $\times 400$ ). (A) Parathyroid tissue section from a rabbit in control groups shows that the positive nuclear rate of PCNA was lower than that in experimental group. (B) Parathyroid tissue section from a rabbit receiving high-phosphate diet for 6 months shows that the positive nuclear rate of PCNA was 99% in experimental groups.

sacrificed in batches of 10 by intravenous injection of 3% sodium pentobarbital (1 mg/kg). The thyroid and parathyroid complexes were surgically removed and immediately fixed with 4% formaldehyde solution for 24–48 hours and were embedded into paraffin.

### Cell count of parathyroid glands

Specimens of the thyroid and parathyroid complexes were immediately fixed in 4% formaldehyde buffer for 24 hours after removal. After conventional paraffin embedding, samples were sectioned into 4  $\mu\text{m}$  thick slices and stained with H&E. The proliferation of parathyroid cells was determined by two experienced pathologists using a light microscope. For the pathological graphic analysis, four regions were randomly selected for each case, the number of parathyroid gland cells in each field of view (FOV) was calculated, and the average number in four FOVs was taken as the number of parathyroid gland cells in each FOV ( $\times 400$  magnification).

### Expressions of glandular PCNA, Bcl-2, and cyclin-D1 proteins

The expressions of PCNA, Bcl-2, and cyclin-D1 proteins in parathyroid cells were detected using immunohistochemistry with the streptavidin-biotin complex method according to manufacturer's instructions. Immunohistochemical staining of PCNA, Bcl-2, and cyclin-D1 was carried out according to the streptavidin-biotin-peroxidase

complex protocol using respective specific rabbit polyclonal antibody, supplied with the immunohistochemical staining kit. Tissues were treated with primary antibody overnight at 4°C. Formalin-fixed, paraffin-embedded normal parathyroid gland served as a positive control, whereas phosphate-buffered saline was used as the substitution of PCNA, Bcl-2, and cyclin-D1 antibody and served as a negative control.

The percentage of positive cells was counted under the light microscope, and four regions were randomly selected for each slide. The total number of glandular cells in each region and the number of cells with positive PCNA, Bcl-2, and cyclin-D1 protein expressions were counted under the pathological graphic analysis system, then the number of positive cells per thousand glandular cells was calculated.

### Immunohistochemistry result scoring

Under a light microscope, the PCNA-positive cells' nuclei appeared as various intensities of brown-yellow. The Bcl-2-positive cells showed brown cytoplasm and fine granular precipitate. Cyclin-D1 protein expression was localized in the nucleus and cytoplasm, and positive cells contained brown granules. The apoptotic cells had dark brown dense nuclei. According to the proportion of positive cells in the cell counts, the specific immune-response intensity was graded: negative (–): <5%; weakly positive (+): 5%–20%; moderately positive (++) : 20%–50%; and strongly

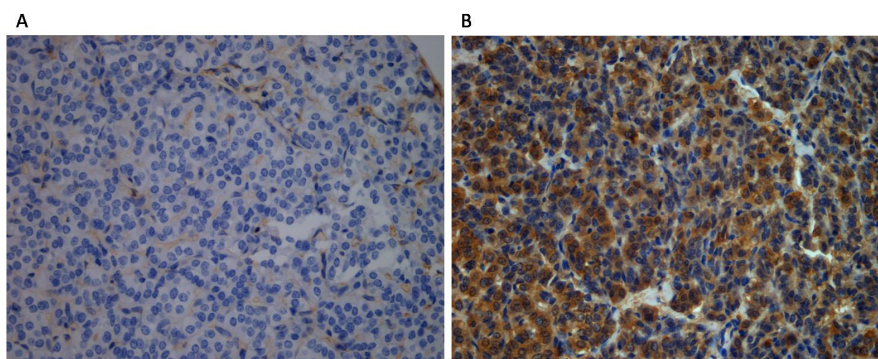


**Figure 3** B cell lymphoma-2 (Bcl-2) protein expression ( $\times 400$ ). (A) Parathyroid tissue section from a rabbit in control groups shows that the positive cytoplasmic expression of Bcl-2 in partial cells. (B) Parathyroid tissue section from a rabbit receiving high-phosphate diet for 6 months with positive cytoplasmic and nuclear expression of Bcl-2 in almost all cells.



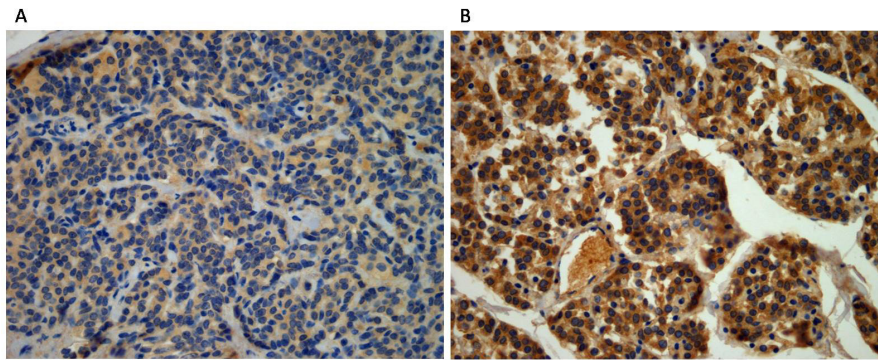


**Figure 4** Cyclin-D1 protein expression (×400). (A) Parathyroid tissue section from a rabbit in control groups shows weak positive cytoplasmic expression of cyclin-D1. (B) Parathyroid tissue section from a rabbit in experimental groups shows strong positive cytoplasmic expression of cyclin-D1.

positive (+++): >50%. Five high-power FOVs (×400 magnification) were randomly selected from each tissue section, photographed, and digitally stored. The HMIAS-2000 color pathological graphic analysis system was used for semi-quantitative analysis. After staining, 200 nucleated cells were counted per FOV under the optical microscope at high magnification for a total of five FOVs. The percentage of positive cells was calculated, and 5% of the positive cells were positive for expression. If the positive cells were scattered (15%–20%), they were considered as +; if they were distributed in sheets (20%–50%), they were considered as ++; and if they were distributed around the glands (50%–80%), they were considered as +++.<sup>8</sup>

#### Quantitative measurement of apoptosis

Specimens of the thyroid and parathyroid complexes were formalin-fixed, dehydrated with graded ethanol, and paraffin-embedded. Sections of 4 μm thickness were prepared for the following experiments.

A DNA-fragment terminal-labeling method (terminal deoxynucleotidyl transferase dUTP nick end labeling) was employed, and the in situ apoptosis detection kit was used according to the manufacturer's instructions. Under the light microscope, four regions were randomly selected from each slide to determine the positive cell ratio. Using the pathological graphic analysis system, the total number of glandular or apoptotic cells in each region was counted, and the number of positive apoptotic cells per 1000 glandular cells was calculated as the AI.

#### Statistical analysis

SPSS V.11.5 (SPSS, Chicago, Illinois, USA) was used for the statistical analyses. Data were presented as mean±SEM, and a Student's t-test was used for the comparison between the experimental and control groups. Univariate analysis of variance was used to analyze the differences between and within the experimental groups. The correlations between protein expression, cell proliferation, and apoptosis were analyzed by Pearson's correlation analysis. The differences were statistically significant with  $p < 0.05$ .

## RESULTS

### Rabbit model of PHPT

The animal model of PHPT was successfully established as previously reported.<sup>7</sup> The study is a continuation of a study conducted in 2012.<sup>7</sup> The immunohistochemical staining is a recent study based on the rabbit model of PHPT.

### Histomorphological examination

#### Hyperplasia of the parathyroid gland

From the end of the third month, subjects in the experimental group showed different degrees of hyperplasia, with a significant increase in parathyroid cell number and parathyroid gland volume (figure 1B). There were no abnormal parathyroid glands in the control group, and thyroid histology showed no change (figure 1A).

#### Cell characteristics and counts in the parathyroid gland

Sixty specimens in the experimental group had hyperplasia of parathyroid cells, and the adipose tissue was completely or mostly replaced with glandular cells, most of which were eosinophilic cells. In some sections, the nuclei of the gland cells were uneven in size, the nucleoli were clear, and the chromatin was loose. The glandular cell count in the experimental group was significantly higher than that in the control group since the second month ( $p < 0.05$ ) (table 1).

#### Expressions of PCNA, Bcl-2, and cyclin-D1 proteins in parathyroid cells

Starting in the second month, the expressions of PCNA, Bcl-2, and cyclin-D1 in parathyroid cells of the experimental group with high-phosphorus diet significantly increased (figures 2B–4B) and were significantly higher than those in the control group ( $p < 0.05$ ) (figures 2A–4A) (table 2).

#### Apoptosis of parathyroid cells

Starting in the second month, the degree of apoptosis of parathyroid cells in the experimental group with high-phosphorus diet (figure 5B) increased significantly and was significantly higher than that in the control group ( $p < 0.05$ ) (figure 5A) (table 2).

**Table 2** Comparison of various parameters between control and experimental groups at 1, 2, 3, 4, 5, 6 months

| Parameter | 1 month          |                  | 2 months          |                  | 3 months          |                  | 4 months          |                  | 5 months           |                  | 6 months           |                  |
|-----------|------------------|------------------|-------------------|------------------|-------------------|------------------|-------------------|------------------|--------------------|------------------|--------------------|------------------|
|           | Control          | Experimental     | Control           | Experimental     | Control           | Experimental     | Control           | Experimental     | Control            | Experimental     | Control            | Experimental     |
| Bcl-2     | 1.059<br>±0.593  | 1.139<br>±0.404  | 1.009<br>±0.712   | 27.769<br>±5.651 | 1.530<br>±0.479   | 32.630<br>±3.138 | 1.843<br>±0.368   | 33.777<br>±4.221 | 2.056<br>±0.593    | 45.024<br>±4.002 | 2.247<br>±0.374    | 51.150<br>±3.951 |
| F<br>(P)  | 0.124<br>0.729   |                  | 220.739<br><0.001 |                  | 959.975<br><0.001 |                  | 568.022<br><0.001 |                  | 1127.729<br><0.001 |                  | 1518.235<br><0.001 |                  |
| PCNA      | 11.314<br>±4.500 | 15.064<br>±4.022 | 9.011<br>±4.393   | 17.484<br>±3.533 | 16.641<br>±2.653  | 23.121<br>±1.764 | 7.276<br>±3.562   | 32.318<br>±3.954 | 10.435<br>±4.077   | 48.328<br>±4.163 | 9.347<br>±2.771    | 55.007<br>±6.958 |
| F<br>(P)  | 3.862<br>0.065   |                  | 22.588<br><0.001  |                  | 41.368<br><0.001  |                  | 221.458<br><0.001 |                  | 422.850<br><0.001  |                  | 371.639<br><0.001  |                  |
| Cyclin-D1 | 0.761<br>±0.327  | 0.961<br>±0.291  | 0.603<br>±0.095   | 1.516<br>±0.417  | 0.804<br>±0.153   | 1.981<br>±0.355  | 0.808<br>±0.252   | 2.633<br>±0.423  | 0.781<br>±0.140    | 3.001<br>±0.571  | 0.836<br>±0.212    | 4.663<br>±0.479  |
| F<br>(P)  | 2.094<br>0.165   |                  | 45.628<br><0.001  |                  | 92.905<br><0.001  |                  | 137.258<br><0.001 |                  | 142.577<br><0.001  |                  | 533.179<br><0.001  |                  |
| TUNEL     | 8.875<br>±2.737  | 11.430<br>±2.954 | 14.253<br>±3.776  | 20.639<br>±3.200 | 16.616<br>±4.541  | 31.065<br>±4.387 | 16.633<br>±2.696  | 42.085<br>±5.718 | 14.845<br>±3.525   | 58.814<br>±5.432 | 17.488<br>±3.897   | 71.893<br>±4.244 |
| F<br>(P)  | 4.026<br>0.060   |                  | 16.648<br>0.001   |                  | 52.372<br><0.001  |                  | 162.088<br><0.001 |                  | 461.067<br><0.001  |                  | 891.412<br><0.001  |                  |

Data are mean±SD.

Bcl-2, B cell lymphoma-2; PCNA, proliferating cell nuclear antigen; TUNEL, terminal deoxynucleotidyl transferase dUTP nick end labeling.

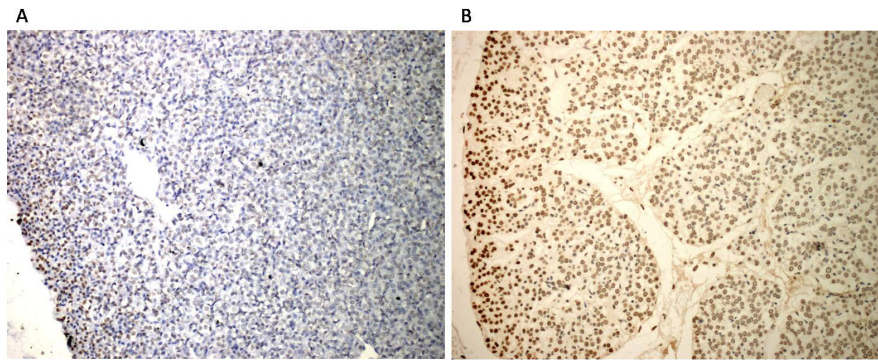


**Figure 5** Image of parathyroid tissue for terminal deoxynucleotidyl transferase dUTP nick end labeling (TUNEL) ( $\times 200$ ). (A) Parathyroid tissue section from a rabbit in control groups shows that positive nuclear rate of TUNEL was 30%. (B) Parathyroid tissue section from a rabbit in experimental groups shows that positive nuclear rate of TUNEL was 90%.

#### Pearson's correlation analysis

In the sixth month, the AI of the experimental group was positively correlated with the glandular cell count and PCNA expression ( $r$  values were 0.671 and 0.645, respectively,  $p < 0.05$ ) (table 3).

#### DISCUSSION

The stability of multicellular organisms is a delicate balance of cell proliferation and apoptosis.<sup>2</sup> Apoptosis and proliferation regulate the cell number homeostasis, and cyclin-D1, PCNA, and Bcl-2 are known to play an important role in regulating cell proliferation and apoptosis.

It has been reported that the main causes of PHPT are parathyroid tumors and excessive proliferation of parathyroid cells.<sup>3</sup> Other studies have shown that cell proliferation, differentiation, apoptosis, and canceration are closely related to the regulation of cell cycle. Cyclin-D1, an important positive regulator of cell cycle, has become the research focus of tumor development. Overexpression of the cyclin gene is the main cause of parathyroid tumors.<sup>5</sup>

In vitro experiments showed that cyclin-D1 was the first cyclin synthesized in the G1 phase, and the expression peaked in the early stages under growth factor stimulation. The overexpression of cyclin-D1 shortens the G1 phase and reduces the cell's dependence on exogenous mitosis, leading to the cell transcription.<sup>9</sup> Therefore, the overexpression of cyclin-D1 results in an imbalance of cell-proliferation cycle, which leads to excessive cell proliferation and tumor cells.<sup>10 11</sup>

There have been few reports on cyclin-D1 and parathyroid hyperplasia.<sup>12–14</sup> Our research showed that high-phosphorus diet caused blood calcium increase and hyperplasia of the parathyroid gland, which significantly increased the PTH concentration in the blood. This result is consistent with

the findings of Demeter *et al.*<sup>15</sup> The animal model of PHPT induced by high-phosphorus diet in this experiment was reliable. However, the rabbit model established in this study only reflects the early stages of PHPT, and changes in the biochemical indicators are early events of the disease.

Our data showed that the proliferation of parathyroid gland cells and the increased cell numbers are correlated with the high expression of cyclin-D1, which is consistent with the previous report.<sup>5</sup> The high expression of cyclin-D1 may promote the proliferation of parathyroid gland cells and play a key role in the pathogenesis of PHPT. Gene therapy might be developed to reduce the cyclin-D1 expression to inhibit the proliferation of parathyroid gland cells in the early stages and prevent parathyroid gland tumor development, as an alternative early treatment for PHPT.

PCNA, a protein that exists only in proliferating cells, is a cofactor of DNA polymerase delta.<sup>2</sup> Our study showed that PCNA expression increased in PHPT gland cells, while the AI significantly increased. The AI was positively correlated with the expression of PCNA, indicating that the balance between apoptosis and proliferation of parathyroid cells was impaired in the PHPT model. Excessive gland cell proliferation led to an increase in the number of gland cells and gland volume.

During adulthood, the low rate of proliferation and apoptosis in normal parathyroid tissues is important for the maintenance of a stable size of parathyroid.<sup>16–19</sup> Cell proliferation and apoptosis are regulated by multiple moleculars. Bcl-2 is the most important anti-apoptotic protein. Studies have shown that Bcl-2 has strong clonogenic ability and potential tumorigenicity, suggesting that increased expression of Bcl-2 in parathyroid glands can induce glandular cell hyperplasia, which may also lead to the glandoma-like growth in nodular tissues. Recent studies have found that abnormal Bcl-2 expression has been reported in studies on PHPT.<sup>20–23</sup> Our results showed that the upregulated expression of Bcl-2 was consistent with the proliferation of parathyroid gland cells, however, it was not negatively correlated with apoptosis, indicating that gland hyperplasia may be the result of a multifactor synergistic effect on cell proliferation and apoptosis.

Starting from the second month, the AI of parathyroid cells increased significantly in the experimental group, which is inconsistent with a rat PHPT model reported by

**Table 3** Correlation of AI and the glandular cell count and PCNA expression in the sixth month

|  |                       | The sixth month |                   |
|--|-----------------------|-----------------|-------------------|
|  |                       | PCNA            | Parathyroid cells |
| AI   | Pearson's correlation | 0.645           | 0.671             |
|  | Sig. (two-tailed)     | 0.044           | 0.033             |
|  | Number                | 10              | 10                |
| AI, apoptosis index; PCNA, proliferating cell nuclear antigen. |                       |                 |                   |



Naveh-Many *et al.* Rat PHPT with renal failure had higher parathyroid cell proliferation rates, whereas apoptosis was not affected.<sup>24 25</sup> The reasons for this inconsistency remain unclear, several hypotheses may explain: first, the duration of the experimental chronic renal failure and the severity of the secondary hyperparathyroidism were substantially lower than those of the experimental PHPT model. Over time, gland hyperplasia may compensatorily increase apoptosis process to avoid excessive parathyroid gland cell proliferation as part of the body's self-protection mechanisms. Second, uncontrolled apoptosis diminishes growth of tissues with benign tumor growth forms, which to some extent limits the rapid increase in gland volume. Third, postproliferation reactivity accelerated the process of apoptosis, and the rat parathyroid glands showed different interspecific tendencies from those of rabbits.

In our study, it was found that the expressions of PCNA, Bcl-2, and cyclin-D1 were significantly upregulated in the PHPT group compared with the control group starting at the end of the second month. Our research demonstrated that all three genes may play important roles in the early stage of PHPT, which has never been reported in previous studies. At the sixth month, the AI of the experimental group was positively correlated with the glandular cell count and PCNA expression, but not Bcl-2, which was different from previous study<sup>26</sup> as well. A possible explanation for this contrary is apoptosis induced by special signaling pathway is independent of Bcl-2 in PHPT rabbit model. The unbalance between proliferation and apoptosis of parathyroid cells impairs cellular homeostasis in parathyroid tissue. There are multitudinous factors affecting apoptosis and cell proliferation. Further studies are needed to investigate the mechanism.

In conclusion, our results revealed that excessive proliferation and apoptosis of parathyroid cells might contribute to the pathogenesis of PHPT, and that PCNA, Bcl-2, and cyclin-D1 might play key roles in this process, although their specific regulatory mechanisms need further investigation. This rabbit PHPT model can be used to study the relationship between cell proliferation and apoptosis in early PHPT lesions, and the related evolution process and regulatory mechanism. This study provides the groundwork for using the rabbit PHPT model to elucidate its pathogenesis and develop treatment strategies.

**Contributors** R-JB is corresponding author who is responsible for concept, design, definition of intellectual content, literature search, experimental studies, data analysis, and statistical analysis. J-TB is responsible for manuscript preparation, manuscript editing, and manuscript review. Other authors are responsible for literature search, experimental studies, and data acquisition. H-LZ and Z-HQ are responsible for specimen collection and preparation of the rabbit model. L-HG is responsible for the pathological graphic analysis. Y-QL, Z-XZ and XC are responsible for manuscript transplantation and review. R-JB is responsible for the overall content as guarantor.

**Funding** This study was supported by the National Natural Science Foundation of China (grant number 82171921, 81071130), Beijing Natural Science Foundation of China (grant number 7202063, 7102082).

**Competing interests** None declared.

**Patient consent for publication** Not applicable.

**Ethics approval** This study was reviewed and approved by the Institutional Animal Care and Use Committee of Beijing Jishuitan Hospital and all experiments were conducted under the biosafety rules of Beijing Jishuitan Hospital.

**Provenance and peer review** Not commissioned; externally peer reviewed.

**Data availability statement** No data are available.

## ORCID iD

Jing-tao Bi <http://orcid.org/0000-0002-1413-7441>

## REFERENCES

- Julia AS, Robert U. New directions in treatment of patient with primary hyperparathyroidism. *Curr Probl Surg* 2003;40:808–49.
- Wang X, Sun B, Zhou F, *et al.* Vitamin D receptor and PCNA expression in severe parathyroid hyperplasia of uremic patients. *Chin Med J* 2001;114:410–4.
- Kaczmarek E, Lacka K, Majewski P, *et al.* Selected markers of proliferation and apoptosis in the parathyroid lesions: a spatial visualization and quantification. *J Mol Histo* 2008;39:509–17.
- Maga G, Hubscher U. Proliferating cell nuclear antigen (PCNA): a dancer with many partners. *J Cell Sci* 2003;116:3051–60.
- Hsi ED, Zukerberg LR, Yang WI, *et al.* Cyclin D1/PRAD1 expression in parathyroid adenomas: an immunohistochemical study. *J Clin Endocrinol Metab* 1996;81:1736–9.
- Draper HH, Sie TL, Bergan JG. Osteoporosis in aging rats induced by high phosphorus diets. *J Nutr* 1972;102:1133–41.
- Bai R-J, Cheng X-G, Yan D, *et al.* Rabbit model of primary hyperparathyroidism induced by high-phosphate diet. *Domest Anim Endocrinol* 2012;42:20–30.
- Yue W, Yang LJ, Ma M. In vivo and in vitro study of the effect of BMP on osteosarcoma. *Chin J Oral Maxillofac Surg* 2000;10:222–4.
- Bai JR, Cleveland JL, Hannink M, *et al.* Phosphorylation-dependent regulation of cyclin D1 nuclear export and cyclin D1-dependent cellular transformation. *Genes Dev* 2000;14:3102–14.
- Imanishi Y, Hosokawa Y, Yoshimoto K, *et al.* Primary hyperparathyroidism caused by parathyroid-targeted overexpression of cyclin D1 in transgenic mice. *J Clin Invest* 2001;107:1093–102.
- Hemmer S, Wasenius VM, Haglund C, *et al.* Deletion of 11q23 and cyclin D1 overexpression are frequent aberrations in parathyroid adenomas. *Am J Pathol* 2001;158:1355–62.
- Tominaga Y, Tsuzuki T, Uchida K, *et al.* Expression of PRAD1/cyclin D1, retinoblastoma gene products, and Ki67 in parathyroid hyperplasia caused by chronic renal failure versus primary adenoma. *Kidney Int* 1999;55:1375–83.
- Hwang TS, Han HS, Hong YC, *et al.* Prognostic value of combined analysis of cyclin D1 and estrogen receptor status in breast cancer patients. *Pathol Int* 2003;53:74–80.
- Guo SS, Wu X, Shimoide AT, *et al.* Frequent overexpression of cyclin D1 in sporadic pancreatic endocrine tumours. *J Endocrinol* 2003;179:73–9.
- Demeter JG, De Jong SA, Oslapas R, *et al.* High phosphate diet-induced primary hyperparathyroidism: an animal model. *Surgery* 1991;110:1053–60.
- Kawata T, Imanishi Y, Kobayashi K, *et al.* Relationship between parathyroid calcium-sensing receptor expression and potency of the calcimimetic, cinacalcet, in suppressing parathyroid hormone secretion in an in vivo murine model of primary hyperparathyroidism. *Eur J Endocrinol* 2005;153:587–94.
- Medici D, Razaque MS, Deluca S, *et al.* FGF-23-Klotho signaling stimulates proliferation and prevents vitamin D-induced apoptosis. *J Cell Biol* 2008;182:459–65.
- White KE, Carn G, Lorenz-Depiereux B, *et al.* Autosomal-dominant hypophosphatemic rickets (ADHR) mutations stabilize FGF-23. *Kidney Int* 2001;60:2079–86.
- Bai X, Miao D, Li J, *et al.* Transgenic mice overexpressing human fibroblast growth factor 23 (R176Q) delineate a putative role for parathyroid hormone in renal phosphate wasting disorders. *Endocrinology* 2004;145:5269–79.
- Miedlich S, Krohn K, Paschke R. Update on genetic and clinical aspects of primary hyperparathyroidism. *Clin Endocrinol* 2003;59:539–54.
- Zhang P, Duchambon P, Gogusev J, *et al.* Apoptosis in parathyroid hyperplasia of patients with primary or secondary uremic hyperparathyroidism. *Kidney Int* 2000;57:437–45.
- Kokawa K, Shikawa T, Otani T, *et al.* Apoptosis and the expression of Bax and Bcl-2 in hyperplasia and adenocarcinoma of the uterine endometrium. *Hum Reprod* 2001;16:2211–8.
- Arnold A, Shattuck TM, Mallya SM. Molecular pathogenesis of primary hyperparathyroidism. *J Bone Miner Res* 2002;17:30–6.
- Naveh-Many T, Rahamimov R, Livni N, *et al.* Parathyroid cell proliferation in normal and chronic renal failure rats. The effects of calcium, phosphate, and vitamin D. *J Clin Invest* 1995;96:1786–93.
- López-Fontana CM, Sasso CV, Maselli ME, *et al.* Experimental hypothyroidism increases apoptosis in dimethylbenzanthracene-induced mammary tumors. *Oncol Rep* 2013;30:1651–60.
- Ma G-L, Bai R-J, Yan D, *et al.* [Relationship between proliferation and apoptosis of parathyroid cell in rabbits with primary hyperparathyroidism]. *Zhonghua Yi Xue Za Zhi* 2011;91:1770–4.